

# Porous silicon upon multicrystalline silicon: Structure and photoluminescence

M. M. MELNICHENKO, K. V. SVEZHENTSOVA

Department for Physics, Taras Shevchenko University, vul. Volodymyrska 64, 03033, Kyiv, Ukraine

E-mail: [carammba@svitonline.com](mailto:carammba@svitonline.com);  
[semiconds-kpi@mail.ru](mailto:semiconds-kpi@mail.ru)

A. N. SHMYRYEVA

National Technical University of Ukraine "KPI", Research Institute of Applied Electronics, Prosp. Peremogy, 37, Kyiv, 03056, Ukraine

E-mail: [ashmyriova@el.ntu-kpi.kiev.ua](mailto:ashmyriova@el.ntu-kpi.kiev.ua)

Ultrathin porous silicon layers have been stain-etched upon multicrystalline silicon (*multi-Si*) substrates. We studied optical and structural properties of porous silicon by photoluminescence, photo-luminescence excitation, reflection, atomic force microscopy and scanning tunnel microscopy methods. It was observed that the thickness of porous silicon did not exceed 20 nm. The photoluminescence method has shown that photoluminescence spectra of porous silicon of different grains have shown that they differ insignificantly ( $\sim 10\%$ ) in intensity. It was found that *por-Si* layers with optimal antireflection characteristics was obtained during etching time 7 min. In the paper the comparison of the reflection characteristics of investigated samples *por-Si* with industrial antireflection coating is presented. © 2005 Springer Science + Business Media, Inc.

## 1. Introduction

Wide use of solar energy requires creation of new technologies and materials enabling reduction of solar cells costs. One of such materials, capable of replacing the expensive monocrystalline silicon (*c-Si*), is multicrystalline silicon (*multi-Si*). Multicrystalline silicon is predicted to become the most common substrate material for photovoltaic cells.

In recent years the interest to the potential application of porous silicon (*por-Si*) in *multi-Si* PV manufacturing technology has considerably increased. The advantages of *por-Si*, such as large active area, reduced reflection losses, capability of widening the bandgap etc. position *por-Si* as a promising material for solar cells technology [1–4]. The use of porous silicon (*por-Si*) is of great interest, as the single technological operation (formation of *por-Si*), required for it, replaces three ones texturization, surface passivation and antireflecting coating (ARC) deposition. As the single-step technique is more industrially applicable, it needs to be investigated thoroughly.

For creating *multi-Si* solar cells the following is crucial: good grain boundaries passivation, increased charge carries life time and good-quality antireflecting coating.

*Por-Si* can be formed in aqueous hydrofluoric solution by two techniques: electrochemical method and chemical (stain) etching method. Both methods are used for formation of *por-Si* antireflection coating on *multi-Si* and *c-Si* solar cells [5, 6]. But the stain etching

method suits better for mass production, because *por-Si* formation process can be controlled by only few external variables (HF concentration, temperature and etching time). Moreover, this method allows to form thin homogeneous *por-Si* layers ( $< 100$  nm), which is very important as the thickness of the *por-Si* layer in solar cells should not exceed the *n-p* junction depth ( $\sim 1$   $\mu\text{m}$ ).

The purpose of the present research was to fabricate ultrathin layers of *por-Si* on *multi-Si* substrates by stain etching and to study their morphological, antireflective and emitting properties.

## 2. Experimental procedure

We used boron doped *multi-Si* square wafers with resistivity of  $1 \Omega\cdot\text{cm}$ , with area of  $100 \text{ cm}^2$  and thickness of  $0.3 \mu\text{m}$ . The samples were cut perpendicularly to the crystalization direction on the wafers. The surface of the wafers was not polished.

Stain etching in HF:HNO<sub>3</sub> lasted for 1–5 min in conditions of room temperature and natural day-time illumination [7].

Morphological analysis of *por-Si* surface was performed by atomic force microscope (AFM) Nanoscope IIIa in "tapping mode" and by scanning tunnel microscope (STM).

Photoluminescence (PL) have been excited by a xenon-150 lamp with a grating monochromator MDR-23 and detected by a photomultiplier FEU-72 through the prism spectrometer IKS-12. The photoluminescence excitation (PLE) spectra was measured at the



Figure 1 Optical contrast image of 3 × 3 cm<sup>2</sup> multi-Si wafer.

PL maximum. All measurements were performed at 300 K.

The reflectance measurements were performed with SPECORD M-40 within the wavelength range of 250–850 nm.

### 3. Results and discussion

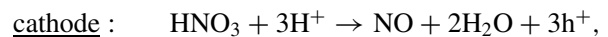
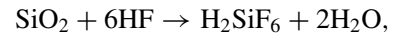
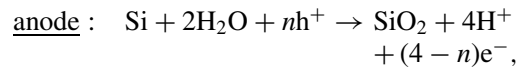
#### 3.1. Stain-etched *por*-Si on multicrystalline silicon

In spite of its increasing use in the photovoltaics industry, multicrystalline silicon is still a relatively poorly understood material, even after twenty years of research [8]. Multicrystalline cell manufacture usually begins with a thermal process in which silicon is melted and solidified in such a way that crystals are oriented in a predetermined direction. A rectangular ingot of multicrystalline silicon at first is cut into blocks or bricks and then finally sliced into thin wafers.

Such *multi*-Si is a complex semiconductor system where the crystalline lattice is interrupted at the grain boundaries and the bulk is often populated by foreign atoms, micro-defects and dislocations. It is fundamentally non-homogeneous, with properties varying over the surface of a wafer and within the volume of an ingot. Wafers of multicrystalline silicon contain many discrete crystals (grains) of silicon, which are clearly visible to the naked eye (Fig.1).

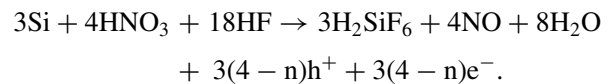
The etching process on *multi*-Si substrates occurs similarly as on *c*-Si ones. At present, it is generally accepted that chemical etching of Si surface in a HF/HNO<sub>3</sub> solution can be considered as a localised

electrochemical process [9]. Microscopically, anode and cathode are formed on the etched surface by the local currents flowing between anode and cathode during etching. Consequently, the chemical etching mechanism should incorporate sources of excess of holes and of electrons in order to describe the charge transfer between the electrodes. The anode reaction consists mainly of the dissolution of Si, while the cathode reaction is a complicated reduction of HNO<sub>3</sub> causing holes to be injected into the Si. The local anode and local cathode reactions are as follows:



where *n*—the average number of holes required for dissolution of one Si atom.

The overall chemical reaction on the Si surface can be described as:



#### 3.2. Structural properties

Morphology of *por*-Si surface obtained by AFM and STM are shown on Fig. 2. It can be seen that *por*-Si has an ordered structure and repeats exactly the morphology of the surface of *multi*-Si substrates, forming pores on every single relief piece.

The method of STM was used for detailed studying separate pores of *por*-Si. Analysis of the obtained images of the surface shows that Si surface is regularly covered with nano-scale hills up to 20 nm high. However, owing to certain sizes of tips the information of the depth can be incorrect as deep narrow pores can be displayed as shallow holes. Therefore thickness of *por*-Si layers has been studied additionally by the method of Auger electronic spectroscopy.

Additional information on *por*-Si thickness was obtained from AES investigation of the layers. Fig. 3 shows typical AES depth profile of the *por*-Si samples. Absence of N and F, which is usual for AES spectra of

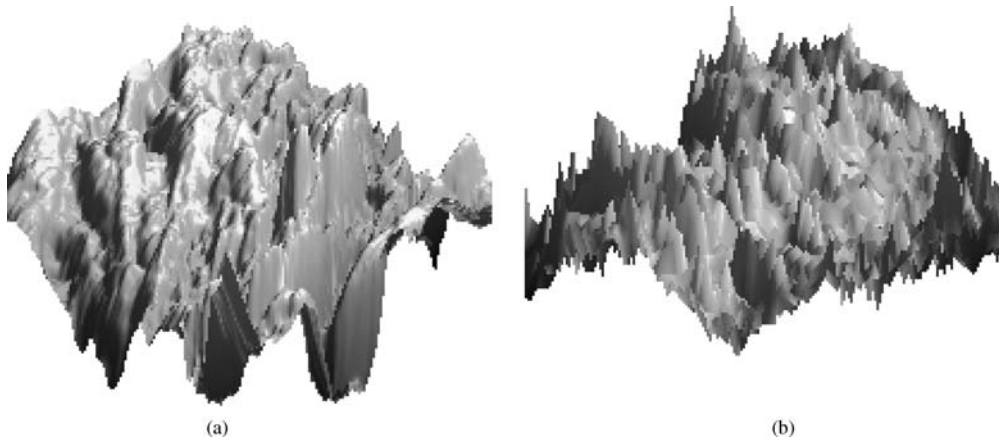


Figure 2 AFM image (a) and STM image (b) of the porous silicon surface (the area of scanning is 3 × 3 μm<sup>2</sup> and 20 × 20 nm<sup>2</sup>, respectively).

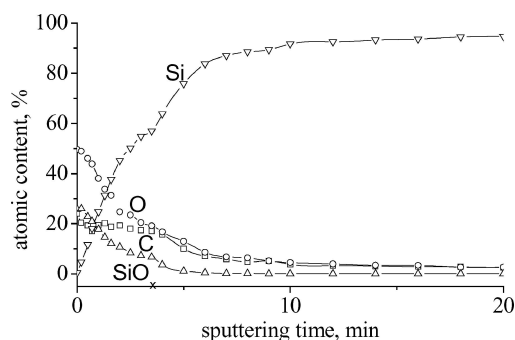


Figure 3 AES depth profile of *por*-Si layers.

stain etching *por*-Si, brings witness of good washing and drying the specimens.

As one can see,  $\text{SiO}_x$  concentration decreases steadily till complete disappearance after 6 min of etching in argon (this corresponds to  $\sim 18\text{--}20$  nm depth, etching rate—3 nm/min). At the same time the concentration of Si increases up to its maximum value at the same depth. So, we conclude that the thickness of nanoporous layer is approximately  $\sim 20$  nm. The O and C signals do not disappear completely, though they fall rapidly at the beginning and their concentrations mean that all O and C are on the surface of silicon substrate.

### 3.3. PL and PLE spectra

The researched *por*-Si layers had bright emission enough to see it with the eye. The PLE spectra are shown on Fig. 4a. PL spectra are excited by the light within the range of 280–530 nm and the maximum of excitation is at  $\sim 320$  nm. PLE as usually has a wide maximum in the visible spectral range and a region of increase of intensity in the near UV range. Fig. 4b shows PL spectra for different grains. As can be seen, each curve is approximately Gaussian with a clear peak at  $\sim 640$  nm. Comparison of photoluminescence spectra of porous silicon of different grains shows that they differ in intensity among themselves insignificantly (only  $\sim 10\%$ ).

Thus, stain etched *por*-Si is formed almost uniformly on the whole area of the *multi*-Si wafer almost independently of the grain orientation, unlike the case of electrochemically etched *por*-Si on multicrystalline Si, which reflects the fact that the *por*-Si formation process exhibits some grain dependent properties. There-

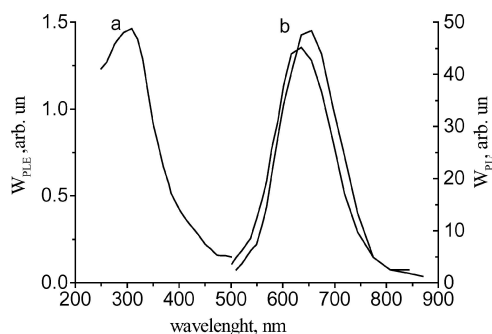


Figure 4 (a) PLE of ultrathin *por*-Si layers received by stain etching on multicrystalline silicon; (b) PL spectra *por*-Si layers for different grains. Excitation wavelength in PL measurements 320 nm.

fore electrochemical etching results in the increase of the difference both in morphology and PL spectra of *por*-Si for differently oriented grains, leading to the formation of a non-uniform *por*-Si layer on multicrystalline Si [2]. This apparently is caused by different mechanisms of *por*-Si growth on different crystal orientation of grains.

### 3.4. Reflection spectra

As it was shown by Fathauer [10] change etching time can form by stain etching *por*-Si layers with different colour. The as-prepared stain-etched *por*-Si samples have grey, darkly grey, brown, dark blue and black under different etching times—4, 4.5, 5, 6 and 7 min accordingly.

Fig. 5 shows the reflectance characteristics of *por*-Si etched for different durations. The reflectivity of a *multi*-Si is presented for comparison. The optimal *por*-Si providing the best reflectance is black *por*-Si. The reflection coefficient decreased, especially, in the short-wave region (280–420 nm). The stain etching process for such *por*-Si formation is characterized by etching time equal to 7 min. As follows from the reflectance characteristics, the duration of the etching affects the location of the minimum of the reflectance.

The reflection spectra of the samples without any antireflection layer and with optimal *por*-Si (black colour) and industrial ARCs in the wavelength range of 250–850 nm are presented on Fig. 6. It can be seen that virtually in the whole investigated range the reflection of the samples with *por*-Si ARC is less, compared to *multi*-Si samples (without ARC) and samples with industrial ARC. Thus the *por*-Si decreases the reflection loss and could be considered as an antireflection coating.

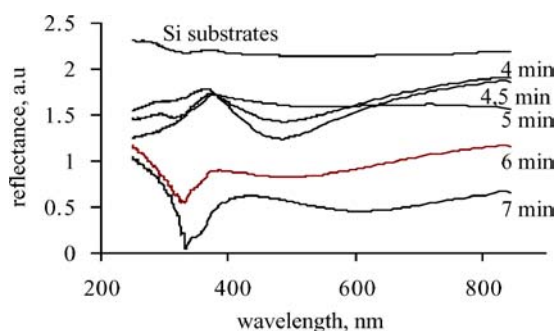


Figure 5 Reflection spectra of *por*-Si samples for different duration's.

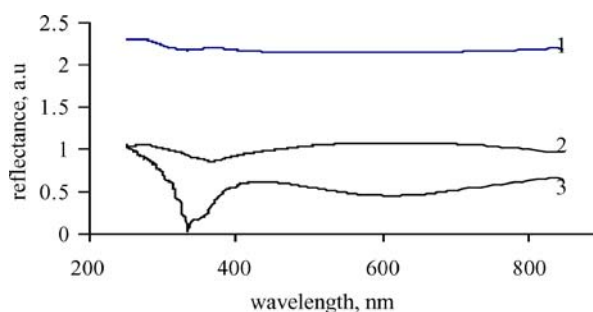


Figure 6 Reflection spectra of samples without ARC and with industrial and *por*-Si ARC. 1- *multi*-Si, 2- industrial ARS, 3- *por*-Si sample (black color).

#### 4. Conclusions

In this work, ultrathin layers of *por*-Si by stain etching (<20 nm) on substrates of very large (100 cm<sup>2</sup>) multicrystalline silicon have been fabricated. Morphological analysis shows clearly that *por*-Si samples have ordered porous structure and the thickness does not exceed 20 nm.

Photoluminescence spectra of the *por*-Si layers have a characteristic gaussian-like shape with a maximum at  $650 \pm 20$  nm. Optimal results with the minimal reflectance are for the black *por*-Si layers formed during 7 min. Comparing the spectra from different layers reveals their difference in intensity. This is apparently caused by the grains different crystallographic orientation and different mechanisms of their growth.

Comparing the reflection characteristics of *por*-Si and industrial ARCs shows that *por*-Si ultrathin layers can be used as ARCs for solar cells.

#### References

1. A. G. CULLIS, L. T. CANHAM and P. D. J. CALCOTT, *J. Appl. Phys.* **82**(3) (1997) 909.
2. S. BASTIDE, A. ALBU-YARON and C. LEVY-CLEMENT, *Solar Energy Mater. Solar Cells* **57** (1999) 393.
3. L. KORE and G. BOSMAN, *ibid.* **57** (1999) 31.
4. R. BILYALOV, L. STALMANS, G. BEAUCARNE, R. LOO, M. CAYMAX, J. POORTMANS and J. NIJS, *ibid.* **65** (2001) 447.
5. S. STREHLKE, D. SATRI, A. KROTKUS, K. GRIGORAS and C. LEVY-CLEMENT, *Thin Solid Films* **297** (1997) 291.
6. R. R. BILYALOV, R. LUDEMANN, W. WETTLING, L. STALMANS, J. POORTMANS, J. NIJS, L. SCHIRONE, G. SOTGUI, S. STREHLKE and C. LEVY-CLEMENT, *Solar Energy Mater. Solar Cells* **60** (2000) 391.
7. S. KALEM and M. ROSENBAUER, *Appl. Phys. Lett.* **67**(17) (1995) 2551.
8. J. LINDMAYER, "Semicrystalline Silicon Solar Cells," in 12th IEEE Photovoltaic Specialists Conf. (1976) p. 82.
9. D. R. TURNER, *Electrochem. Soc.* **107** (1960) 810.
10. R. W. FATHAUER, T. GEORGE, A. KSENDZOV and R. P. VASQUER, *Appl. Phys. Lett.* **60** (1992) 995.